Hydration of nitriles to amides in water by SiO₂-supported Ag catalysts promoted by adsorbed oxygen atoms

Ken-ichi Shimizu [a,*], Naomichi Imaiida [b], Kyoichi Sawabe [b], Atsushi Satsuma [b]

[a] Catalysis Research Center, Hokkaido University, N-21, W-10, Sapporo 001-0021, Japan
[b] Department of Molecular Design and Engineering, Graduate School of Engineering, Nagoya University, Nagoya 464-8603, Japan

ABSTRACT

A series of silica-supported silver catalysts with similar Ag loading (5 or 7 wt%) but with different preparation methods (calcination in air and reduction by H₂ or NaBH₄) were prepared, and their structure was characterized by microscopy (STEM), X-ray absorption fine structure (XAFS), and CO-titration of surface oxygen atom. Ag is present as metal nanoparticle with a size range of 17–30 nm. Their surface was partially covered with oxygen atoms, and the surface coverage of the oxygen depends on the preparation condition. For hydration of 2-cyanopyridine as a test reaction, turnover frequency (TOF) per surface Ag species is estimated. TOF does not show a good correlation with Ag particle size, but it linearly increases with the coverage of the surface oxygen atoms on Ag particles. The Ag/SiO₂ catalyst prepared by H₂ reduction at 700 °C shows the highest TOF and it acts as effective and recyclable heterogeneous catalyst for selective hydration of various nitriles to the corresponding amides. Kinetic and Raman spectroscopic studies suggest that the surface oxygen atom adjacent to Ag⁰ sites plays an important role in the dissociation of H₂O.

1. Introduction

Hydration of nitriles to the corresponding amides is an important transformation from both organic chemistry and industrial points of view. Conventional methods of nitrile hydration with strong acid or base catalysts have drawbacks such as overhydrolysis of amides into carboxylic acids and the formation of salts after neutralization of the catalysts [1]. Homogeneous catalytic systems using complexes [2–7] and colloids [8,9] of transition metals under neutral conditions have been reported. However, they have disadvantages such as difficulty in catalyst/product separation, use of organic solvent, high price of ligands and platinum group metals, and low activity for hydration of heteroaromatic nitriles because of their strong coordination to the metal centers. Use of recyclable heterogeneous catalyst in water is an ideal system from environmental and practical viewpoints [10–18]. Previously, Sugiyama et al. [11] reported that hydration of acrylonitrile by SiO₂-supported Ag catalyst gave 100% selectivity to acrylamide at 75 °C, though its activity was much lower than other metal catalysts. Mitsudome et al. [15] developed hydroxyapatite-supported Ag nanoparticles (AgHAP) which effectively catalyzed the selective

hydration of aromatic and heteroaromatic nitriles, though the catalyst was not effective for less reactive aliphatic nitriles.

Unsupported or supported large Ag particles are well established catalysts for partial oxidation reactions and are the commercial catalysts for production of ethylene oxide and formaldehyde [19]. Salts of Ag(I) are effective homogeneous Lewis acid catalysts in organic synthesis [20]. In the research area of organic synthesis, however, less attempts have been focused on catalytic properties of metallic Ag species [15,21,22] (nanoparticles and nanoclusters) compared with well known catalysts based on platinum-group-metals, Ni, Cu, and Au. Our group has paid attention to unique catalytic properties of Ag clusters for a series of organic reactions involving C—H and H—H activation as a key step, such as dehydrogenation of alcohols, one-pot C—C and C—N bonds formation reactions using alcohols, and selective hydrogenation. We have found general tendencies that Ag clusters with size below a few nanometers give higher TOF than larger Ag nanoparticles, which indicates that coordinatively unsaturated Ag atom plays an important role [22]. In contrast, Mitsudome et al. [15,21] reported that relatively large Ag nanoparticles (7.6 nm) on HAP showed significantly high activity for selective hydration reactions (silanes to silanols and nitriles to amide). These findings lead us to hypothesize that relatively large Ag metal particles may have a specific site for dissociative activation of water. However, experimental and theoretical studies of water adsorption on Ag surfaces have established that water dissociation does not occur on clean Ag surfaces [23,24] but occurs on the Ag surface precovered with oxygen

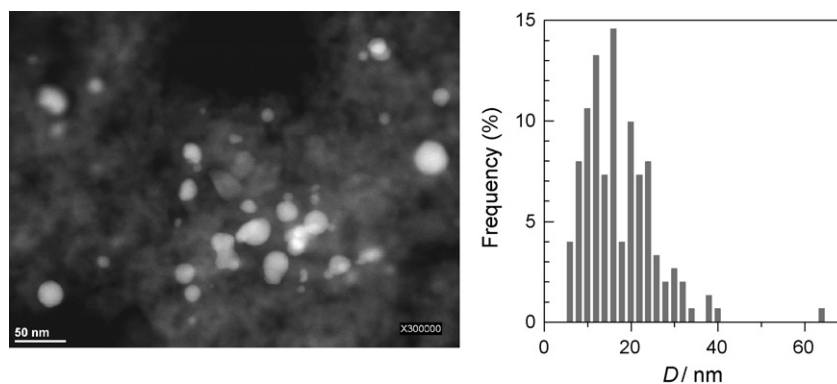**Fig. 1.** A STEM image and particle size distribution of Ag/SiO$_2$-17.

atoms (O$_{ad}$) to yield surface OH species [25–28]. On the other hand, some of the homogeneous [2–7] and heterogeneous [12] catalysts effective for the selective hydration of nitriles employed a design concept of so-called "bifuctional catalysis"; cationic metal center acts Lewis acid, activating the nitrile molecule, and the ligand acts as a Brønsted base, generating the nucleophile (OH$^-$ group). Based on these reports, we assumed that hydration of nitriles by Ag metal particles catalyst could be promoted by O$_{ad}$ which could act as co-catalyst for dissociative activation of H$_2$O. We report herein that SiO$_2$-supported Ag nanoparticles partially covered with O$_{ad}$ act as effective and recyclable heterogeneous catalysts for in this reaction. Kinetic studies and the effect of the O$_{ad}$ coverage on TOF are studied to discuss a catalyst design concept.

2. Experimental

SiO$_2$ (Q-15, 198 m^2 g^{-1}) was supplied from Fuji Silysia Chemical Ltd. The Ag(I)-loaded precursor was prepared by impregnating SiO$_2$ (10 g) with an aqueous solution of silver nitrate (0.046 M) followed by evaporation to dryness at 80 °C, and by drying at 100 °C for 20 h. A series of SiO$_2$-supported silver catalysts with different silver particle size (D/nm, denoted as Ag/SiO$_2$-D), were prepared by calcination of the Ag(I)-loaded precursor in an oven under air, followed by reduction in a flow of 1% H$_2$/He (flow rate of 100 cm^3 min^{-1}) for 10 min, followed by exposing the catalyst to air at room temperature. The catalyst named Ag/SiO$_2$-17B was prepared by reducing the Ag(I)-loaded precursor (5 g) with aqueous solution (10 g) of NaBH$_4$ (0.04 g) at 30 °C for 0.5 h, followed by centrifugation and by washing with water until the pH of the solution was below 8. The Ag loading, temperatures of calcination (T$_{cal}$) and reduction (T$_{H2}$) and the average metal particle size are summarized in Table 1. Ag/SiO$_2$-17 was used as a standard catalyst.

High angle annular dark field scanning TEM (HAADF-STEM) image was recorded using a HD-2300S (Hitachi) microscope operated at 200 kV. Transmission electron microscopy (TEM) measurement was carried out using a JEOL JEM-2100F TEM operated at 200 kV.

X-Ray diffraction (XRD) patterns of the powdered catalysts were recorded with a Rigaku MiniFlex II/AP diffractometer with Cu Kα radiation. Average metal particle size was calculated from the half-width of the Ag (1 1 1) peak at 38.1° in the XRD pattern using Scherrer equation.

The number of oxygen atoms on the catalysts was estimated from the number of CO$_2$ molecules formed by the reaction of CO + O$_{ad}$ = CO$_2$ at 350 °C. The catalysts (stored under air at room temperature) was placed in a fixed-bed flow reactor (inner diameter = 4 mm) at 350 °C under a flow of He. Then, the catalyst was exposed to a flow of 0.4%CO/He at a flow rate of 100 cm^3 min^{-1}, and the effluent gas was continuously analyzed by nondispersive

infrared CO/CO$_2$ analyzers (Horiba VIA510). Note that CO$_2$ might be produced via the water-gas shift reaction (CO + H$_2$O = CO$_2$ + H$_2$). In a separate experiment using Ag/SiO$_2$-17, a possible formation of H$_2$ during the above reaction of O$_{ad}$ with CO at 350 °C was checked by on-line mass spectroscopy (BEL Mass, BEL Japan, Inc.). The result showed no formation of H$_2$, which confirmed that the determination of the number of O$_{ad}$ with our method was adequate.

Raman spectra, with a resolution of 3 cm^{-1}, were collected at room temperature with a NRS-1000 Raman spectrometer equipped with a microscope and a 532.3 nm laser as an excitation source. Two scans were accumulated, and each scan required 7 min. Powders of a freshly prepared Ag/SiO$_2$-17 (ca 10 mg) was immediately placed on a glass plate under ambient condition, and a Raman spectrum was measured ex situ. Then, H$_2$O (ca 50 mg) was dropped to the sample, and Raman spectrum was measured under ambient condition. After 45 min, the spectrum of the dry Ag/SiO$_2$-17 sample was measured.

Commercially available organic compounds (from Tokyo Chemical Industry or Kishida Chemical) were used without further purification. The GC (Shimadzu GC-14B) and GCMS (Shimadzu GCMS-QP2010) analyses were carried out with Ultra ALLOY capillary column (Frontier Laboratories Ltd.) using nitrogen or He as the carrier gas.

For catalytic tests, Ag/SiO$_2$-17 (45 mg, 3 mol% Ag with respect to nitrile), nitrile (1 mmol) and water (2 g) were added to a pyrex reaction vessel equipped with a condenser. After being sealed with a rubber cap, the vessel was heated at 140 °C under air. The reaction mixture was refluxed and was stirred at 500 rpm. Note that 2-cyanopyridine was not completely dissolved in water at room temperature, but it was dissolved in water at 140 °C. After the reaction, the reaction mixture was analyzed by GC. Products were identified with GCMS and GC using commercial amides and carboxylic acids as standard compounds. After the reaction, methanol (co-solvent) and small amount of n-hexanol (internal standard) were added to the reaction mixture, and conversion of a nitrile and yields of products were determined by GC. In separate catalytic experiments, after complete conversion of nitriles, methanol (6 mL) was added to the reaction mixture, and then Ag/SiO$_2$-17 was removed by centrifugation. The solution was evacuated at 50 °C to give the crystalline product, which was identified by ^{1}H-NMR (see the Supporting Information).

3. Results and discussions

3.1. Characterization of SiO$_2$-supported Ag species

A representative STEM micrograph and Ag particle size distribution of a representative catalyst (Ag/SiO$_2$-17) are shown in Fig. 1. The particle size analysis, conducted on 151 particles, shows an

Table 1
List of catalysts.

Catalysts-D[a]	Ag loading (wt%)	T_{cal}[b]/°C	T_{H2}[c]/°C	D[a]/nm	O_{ad} coverage[d] (%)
Ag/SiO$_2$-30	5	900	–	30.3	5
Ag/SiO$_2$-25	5	500	900	25.4	4
Ag/SiO$_2$-17	7	500	700	17.5 (17.4)[e]	22
Ag/SiO$_2$-17B	7	500	(NaBH$_4$)[f]	16.9	7

[a] Average particle size (nm) of supported metal estimated by XRD using the Scherrer formula.
[b] Temperatures of calcination.
[c] Temperatures of reduction in 1% H_2/He(5 min).
[d] Coverage of surface oxygen atom (O_{ad}) on Ag metal particle. The number of surface Ag atom was estimated from the particle size, and the number of O_{ad} was estimated by its reaction with CO to CO_2 at 350 °C.
[e] Average Ag particle size was estimated from STEM analysis.
[f] Ag(I) species in the catalyst was reduced by aqueous solution of NaBH$_4$.

average size of 17.4 ± 8.2 nm. The extended X-ray absorption fine structure (EXAFS) showed the formation of metallic Ag (Figs. S1 and S2, Table S1). The XRD result of Ag/SiO$_2$-17 (not shown) showed a diffraction line at 38.1° due to Ag metal. The average size of Ag crystallites estimated using Scherrer equation is 17.5 nm, which is nearly consistent with the size from STEM analysis.

It is reasonable to assume that the surface of the SiO$_2$ support is not reduced by CO at 350 °C. Thus, the number of oxygen atoms on the Ag metal surface, $[O_{ad}]$, can be estimated from the number of CO_2 molecules formed by the reaction of $CO + O_{ad} = CO_2$ at 350 °C. Although the catalyst was prepared by H_2 reduction of a pre-calcined catalyst at 700 °C, O_{ad} could be formed on Ag after exposing the reduced catalyst to ambient condition. The number of surface Ag atoms, $[Ag_S]$, was estimated from the average Ag particle size (from XRD analysis). Using the numbers of surface Ag atoms and O_{ad}, the surface coverage of O_{ad} (θ_O) defined as $\theta_O = [O_{ad}]/[Ag_S] \times 100$ was estimated (Table 1). Note that Ag/SiO$_2$-17B, prepared by liquid phase reduction by NaBH$_4$, has nearly the same Ag size with Ag/SiO$_2$-17 but has lower O_{ad} coverage.

By changing the temperatures of calcination and H_2 reduction, Ag/SiO$_2$–25 and Ag/SiO$_2$–30 were prepared. XRD patterns of these samples and Ag/SiO$_2$-17B showed diffraction lines due to Ag metal. It is shown that Ag species in the catalysts shown in Table 1 are metallic Ag, which implies that bulk structure of Ag does not depend on the preparation condition. The average size of Ag metal crystallites estimated by Scherrer equation and the surface coverage of O_{ad} are listed in Table 1.

3.2. Structure–activity relationship

We carried out hydration of 2-cyanopyridine in water at 140 °C as a model reaction. Considering the previous result by Sugiyama et al. that Ag/SiO$_2$-catalyzed hydration of a nitrile to amide at low temperature (75 °C) resulted in low yield of amide (1.5%) [11], we adopted a relatively high reaction temperature (140 °C). The catalytic results for various Ag catalysts are compared in Table 2. 2-Picolinamide as a desired product was selectively produced by these catalysts. The initial rate of the amide formation was measured under the condition where the conversion was below 30%. Among various Ag/SiO$_2$ catalysts, Ag/SiO$_2$-17 showed the highest rate of amide formation. Ag powder showed lower reaction rate than Ag/SiO$_2$-17. Consequently, Ag/SiO$_2$-17 was found to be the most active catalyst.

Using the initial rate in Table 2 and the number of surface Ag atoms, TOF per surface Ag species was calculated. For a series of Ag/SiO$_2$ catalyst, the TOF is plotted as a function of the diameter of Ag nanoparticles in Fig. 2. There is no clear relation between TOF and the particle size. In contrast, as shown in Fig. 3, the TOF depended strongly on the coverage of O_{ad}. TOF increases with increase in the surface coverage of O_{ad}, and the Ag/SiO$_2$-17 catalyst shows the highest TOF.

Table 2
Catalytic hydration of 2-cyanopyridine in water.[a]

Catalysts	Conv. (%)	Yield. (%)	Rate[b]/mmol g$_{-Ag}$$^{-1}$ h^{-1}	TOF[c]/h^{-1}
Ag/SiO$_2$-30	8	6	83	208
Ag/SiO$_2$-25	14	4	41	81
Ag/SiO$_2$-17B	25	25	222	285
Ag/SiO$_2$-17[d]	41	37	513	667
Ag powder[e]	9	8	13	24
SiO$_2$[f]	3	2	–	–

[a] Conditions: 2-cyanopyridine (1.0 mmol), H_2O (3 g), catalyst (0.01 mmol Ag), $t = 1$ h, $T = 140$ °C. Conversion and yield of 2-picolinamide were determined by GC.
[b] Initial rate of the formation of 2-cyanopyridine per gram of Ag in the catalyst measured under the condition in which conversions were below 50%.
[c] TOF calculated using the number of surface Ag atom and the initial rate.
[d] $t = 0.4$ h.
[e] catalyst (0.06 mmol Ag).
[f] SiO$_2$ = 0.02 g.

3.3. Catalytic performance of SiO$_2$-supported Ag

Next, the scope of nitriles for the reaction catalyzed by Ag/SiO$_2$-17 was examined. As shown in Table 3, the present hydration method showed substrate generality with respect to aliphatic, aromatic, heteroaromatic, and α,β-unsaturated nitriles. Hydration of 2-cyanopyridine at 140 °C for 3 h gave 2-picolinamide with 98% yield (entry 1). After the hydration of 2-cyanopyridine (entry 1), the catalyst was retrieved from the reaction mixture by centrifugation. After washing the removed catalyst with water followed by drying in air at for 12 h, the catalyst showed a lower amide yield (83%) under the same condition. TEM measurement of the Ag/SiO$_2$-17 catalyst after the first cycle showed an average Ag size of 20.8 ± 14.3 nm (Figs. S3 and S4). The size and distribution were increased by the reaction. This will be one of the main reasons of
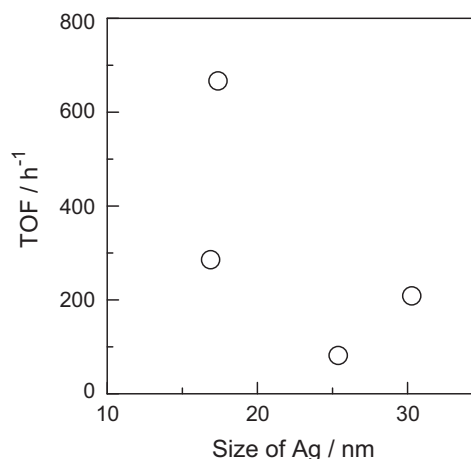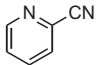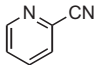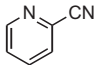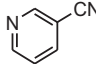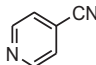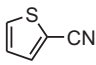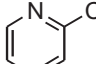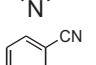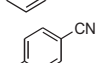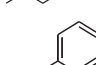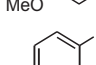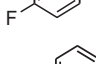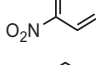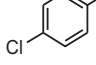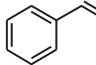

Fig. 2. TOF based on the number of surface Ag atom vs particle size of Ag in Ag/SiO$_2$.

Table 3
Hydration of various nitriles under various conditions by Ag/SiO$_2$-17.[a]

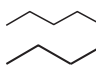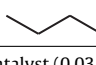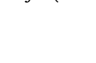| Entry	Nitrile	t/h	T/°C	Yield (%)
1	(2-cyanopyridine)	3	140	98
2[b]				91
3[c]				92
4	(3-cyanopyridine)	9	160	91
5	(4-cyanopyridine)	12	160	96
6	(2-thiophencarbonitrile)	3	160	94
7	(pyrazinecarbonitrile)	0.5	140	92[d]
8[e]		48		85[d]
9	(benzonitrile)	48	160	57
10	(4-methylbenzonitrile)	48	160	55
11	(4-methoxybenzonitrile, MeO)	48	160	69
12	(4-fluorobenzonitrile, F)	48	160	94
13	(4-nitrobenzonitrile, O$_2$N)	12	160	95
14	(4-chlorobenzonitrile, Cl)	40	160	95
15	(cinnamonitrile)	15	160	92
16[g]	(aliphatic nitrile)	48	160	71(7[f])
17[g]	(aliphatic nitrile)	24	160	86
18[g]	(aliphatic nitrile)	48	160	90

[a] Conditions: nitrile (1 mmol), catalyst (0.03 mmol Ag), water (2 g). Conversion and yield of amides were determined by GC.

[b] Reuse 1.

[c] Reuse 2.

[d] Isolated yield of the amide.

[e] Conditions: nitrile (5 mmol), catalyst (0.0025 mmol Ag), water (2 g).

[f] Yields of the corresponding carboxylic acid.

[g] catalyst (0.09 mmol Ag).
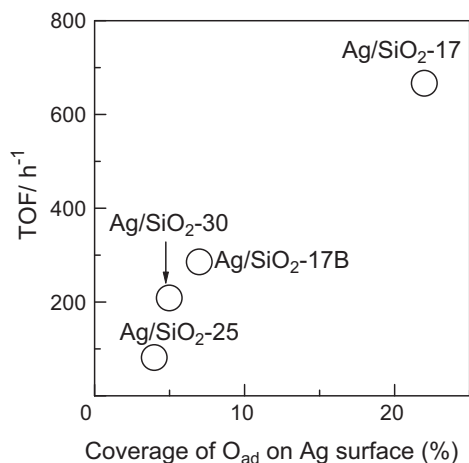
Fig. 3. TOF based on the number of surface Ag atom vs coverage of the surface oxygen on Ag metal particle.

a decrease in the catalytic activity. However, after calcination of the recovered catalyst at 500 °C for 0.5 h, followed by reduction in 1% H$_2$/He at 700 °C for 10 min, the recovered catalyst was reused at least two times without marked loss of its catalytic activity (entries 2, 3).

Other heteroaromatic nitriles such as 3-cyanopyridine, 4-cyanopyridine, 2-thiophencarbonitrile and prazinecarbonitrile (entries 4–7) and aromatic nitriles (entries 9–14) were also selectively hydrated to the corresponding amides in moderate to high yield (55–99%). The α,β-unsaturated nitrile, cinnamnitrile, was selectively hydrated to afford the corresponding α,β-unsaturated amide (entry 15). Notably, the less reactive aliphatic nitriles were also hydrated to the corresponding aliphatic amides in good to high yield (entries 16–18). A larger scale reaction (entry 8) of prazinecarbonitrile (6 mmol) with small amount of Ag/SiO$_2$-17 (Ag = 0.3 mmol, 0.05 mol%) for 48 h gave 85% isolated yield of the corresponding amide (turnover number of 1750), after the separation of the catalyst, followed by evaporation of the filtrate. No by-products were observed by GC and ^{1}H NMR analyses.
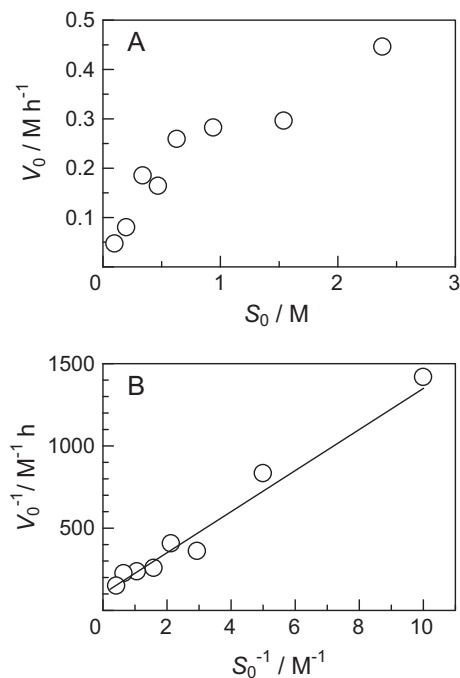
Fig. 4. (A) Rate dependence on the 2-cyanopyridine concentration, and (B) Lineweaver–Bruk plot. Conditions: 2-cyanopyridine (0.045–3.2 M), Ag/SiO$_2$-17 (0.01 mmol Ag), H$_2$O (3 g), 140 °C.

3.4. Kinetic and mechanistic studies

To discuss the mechanism, we carried out kinetic studies for the hydration of 2-cyanopyridine by Ag/SiO$_2$-17. First, we examined the dependence of the reaction rate on the 2-cyanopyridine concentration (Fig. 4A). Initially, the rate of amide formation linearly increases with an increase in the concentration of the nitrile (0–0.6 M) and then levels off at higher concentration. A good linear correlation is observed in a Lineweaver–Burk plot (Fig. 4B), indicating that the reaction follows Michaelis–Menten-type kinetics: $V_0^{-1} = a + b \cdot S_0^{-1}$ ($a = 1.5$ h M^{-1}, $b = 1.9$ h), where S_0 is the initial concentration of 2-cyanopyridine and V_0 is the initial rate of amide formation. This suggests that the free nitrile and an adsorption site on the silver catalyst are in equilibrium with the nitrile-Ag adsorption complex as a reaction intermediate, which is then irreversibly converted to give the product and the latter step is the rate-limiting step. Note that a plot of S_0/V_0 vs S_0 (Fig. S5) does not give a linear correlation, indicating that the mechanism does not fit to Langmuir–Hinshelwood type of equation. Kinetic isotope effect, defined as the ratio of the rate with 2-cyanopyridine/H$_2$O and 2-cyanopyridine/D$_2$O mixtures (r_H/r_D), was studied at 140 °C. Note that the initial rate with H$_2$O and D$_2$O (r_H and r_D) were measured under the same conversion level (41%). The result showed a secondary kinetic isotopic effect ($r_H/r_D = 1.3$). This indicates that H$_2$O dissociation on the catalyst is kinetically important, but some elementary steps other than O—H dissociation are kinetically more relevant. Arrhenius plots for the hydration of 2-cyanopyridine (in a temperature range of 25–140 °C) and pyrazinecarbonitrile (25–120 °C) in water by Ag/SiO$_2$-17 are shown in Fig. S6. Apparent activation energies for the reaction of 2-cyanopyridine and pyrazinecarbonitrile were 48 and 44 kJ mol^{-1}.

Next, we examined the relationship between the relative rates and the Hammett parameter (σ) for the hydration of benzonitriles (Fig. 5). To study the substituent effect, hydration of benzonitrile derivatives were tested under the condition shown in Fig. 5 where all derivatives were dissolved. It was found that substituents bearing electron-withdrawing groups were more reactive than those
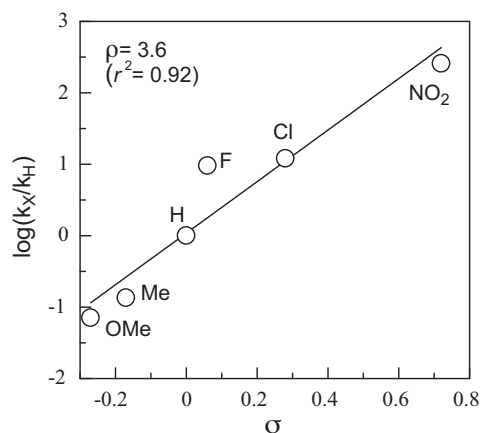

Fig. 5. Hammett plot for hydration of p-substituted benzonitriles. Conditions: nitrile (0.1 mmol), Ag/SiO$_2$-17 (0.1 mmol Ag), H$_2$O (3.0 g), 140 °C.

bearing electron-donating groups. There is a fairly good linearity between $\log(k_X/k_H)$ and σ giving a positive slope ($\rho = 3.6$), indicating that a transition state in the rate-limiting step of the catalytic reaction have a negative charge at the α-carbon atom adjacent to the phenyl group. Taking the Michaelis–Menten-type kinetics (Fig. 4B) and the relatively low kinetic isotope effect ($r_H/r_D = 1.3$) into account, the positive ρ value suggests that nucleophilic addition of OH$^{\delta-}$ species to the nitrile carbon atom of adsorbed nitrile species via a negatively charged transition state is the rate-limiting step.

Previous density functional theory (DFT) calculations established that water dissociation on clean Ag surfaces around 140–160 °C is unfavorable from both kinetic and thermodynamic viewpoints [23,24]. Zhang and Whitten reported that the H$_2$O adsorption energies for the atop, bridge and hollow sites on the surface of Ag$_{31}$ cluster is 0.14, 0.19, and 0.24 eV [23]. These values are comparable to the hydrogen bond energy between H$_2$O molecules (0.22 eV) [29], indicating that H$_2$O weakly adsorbs on the clean Ag surfaces. Gomes et al. recently reported systematic DFT studies on water dissociation on the surfaces of various metals (Co, Ni, Cu, Ru, Rh, Pd, Ag, Ir, Pt, Au) and showed that Ag was the least reactive metal from both kinetic and thermodynamic viewpoints. Gibbs free energy for the water dissociation at 190 °C on Ag(1 1 0) is calculated to be +121.4 kJ mol^{-1} [24]. However, a DFT study by Montoya and Haynes [25] showed that H$_2$O dissociates more readily on an oxygen-dosed Ag(1 1 1) surface as opposed to a clean Ag(1 1 1) surface because pre-existing oxide provides a low-barrier route to surface products. Heat of reaction for water dissociation on the oxygen-dosed Ag(1 1 1) surface was calculated to be −86.5 kJ mol^{-1} [25]. The DFT study by Wang et al. [26] demonstrated that oxygen atom-preadsorbed Ag surface had higher activity in O—H bond cleavage of water than clean Ag surface. According to linear free energy (Brønsted-Evans-Polanyi) relationships widely observed in heterogeneous catalysis [24,26,30], it is expected that the reaction barrier for the water dissociation on the oxygen atom-adsorbed Ag surface is significantly lower than that on the clean Ag surface. Experimentally, water dissociation on clean and oxygen precovered Ag surfaces has been one of the popular system in the research area of surface science [27,28]. Oxygen atom (O$_{ad}$) covered Ag metal surfaces have proved to be highly reactive for water dissociation; the formation of OH has been observed above 200 K, following the reaction path of H$_2$O + O$_{ad}$ → 2OH$_{ad}$ [27]. Hydrogen bond between O$_{ad}$ and a H atom in H$_2$O plays an important role in this reaction [28].

To give a direct evidence on the OH formation over Ag/SiO$_2$-17, ex situ Raman spectroscopy was employed. Fig. 6 shows changes in the Raman spectra of Ag/SiO$_2$-17 during successive treatments.
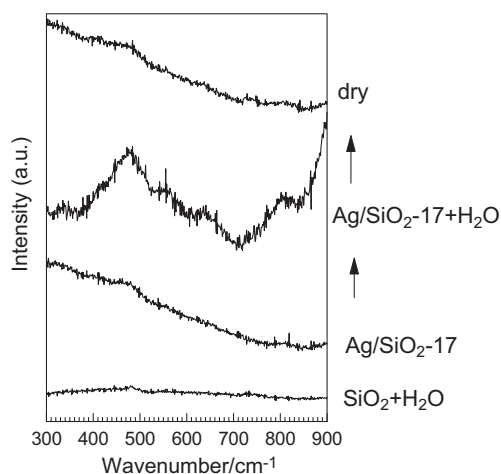
Fig. 6. Raman spectra of Ag/SiO$_2$-17 and SiO$_2$.

When Ag/SiO$_2$-17 (ca 10 mg) was soaked with water (ca 50 mg), new bands centered round 480 and 810 cm^{-1} and shoulder bands around 550 and 640 cm^{-1} were observed. The bands at 480 and 550 cm^{-1} can be assigned to Ag—O stretching vibration of adsorbed OH on Ag, and the bands at 810 cm^{-1} can be assigned to AgO—H bending vibration of adsorbed OH [31–34]. Treatment of SiO$_2$ with water in the same manner did not result in the appearance of these bands. After subsequent drying of the wet Ag/SiO$_2$-17 sample for 45 min under ambient condition, the state of the sample was changed from wet slurry to dry powder, and the Raman bands due to AgOH species were nearly absent. These results show that water dissociation occurs on the Ag metal surface of Ag/SiO$_2$-17, following the reaction path H$_2$O + O$_{ad}$ → 2OH$_{ad}$, but the OH$_{ad}$ species are unstable under the ambient condition.

Based on the above-mentioned facts and our mechanistic results, a possible reaction mechanism of nitrile hydration by Ag/SiO$_2$-17 is shown in Fig. 7. Nitrile and the catalyst surface are in equilibrium with the nitrile-Ag adsorption complex (step 1). The O$_{ad}$ site as a Brønsted base abstracts proton from H$_2$O, resulting in the formation of H$^{\delta+}$ on the O$_{ad}$ site and HO$^{\delta-}$ on the Ag site (step 2). Nucleophilic addition of OH$^{\delta-}$ species to the nitrile carbon atom of adsorbed nitrile species occurs to give the amide. This step, as the rate-limiting step, occurs via a negatively charged transition state (step 3). There might be a possibility that the surface of SiO$_2$ support is involved in the mechanism, such as adsorption of nitriles. Further mechanistic study is in progress to clarify the mechanism.

Recently, surface oxygen-enhanced reactivity of precious metal surfaces toward water dissociation has been confirmed using DFT calculations or surface science techniques [26,35–37]. For example, Shavorskiy et al. reported that small amount of adsorbed oxygen induced dissociation of water on the surface of five metals (Ru, Rh, Pd, Ir, Pt) [36]. The O$_{ad}$-enhanced reactivity of precious metal
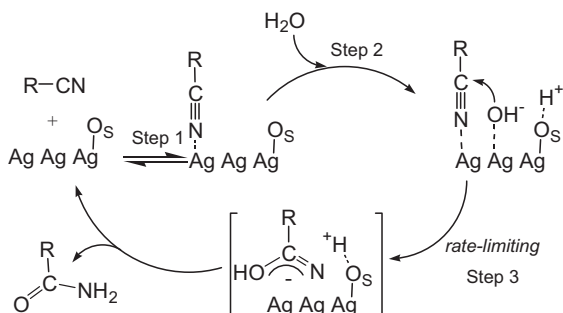
surfaces has been confirmed in several systems using surface science techniques [38,39]. Gong and Mullins [38] and Friend and co-workers [39] independently reported that an oxygen atom on Au(1 1 1) acted as basic co-catalyst that promotes various organic reactions at low temperatures. These examples, coupled with findings in the present study, suggest that cooperation of metal surface and the surface oxygen as a basic co-catalyst may open new possibilities for the tailoring of supported metal catalysts for green organic reactions.

4. Conclusion

Based on the well established fact that oxygen-adsorbed Ag surfaces show higher reactivity for water dissociation than clean Ag surfaces, we have developed the SiO$_2$-supported Ag particles with the surface oxygen atoms (O$_{ad}$) as a highly effective heterogeneous catalyst for hydration of nitriles. A linear correlation between TOF and the coverage of O$_{ad}$ is shown, which indicates that O$_{ad}$ is indispensable for this catalytic system. The Ag/SiO$_2$ catalyst with Ag size of 17 nm and oxygen coverage of 22% shows the highest TOF.

The catalyst has a high synthetic utility, because it is reusable and shows high activity for selective hydration of aliphatic, aromatic, heteroaromatic, and α,β-unsaturated nitriles to the corresponding amides. Fundamental studies suggest a cooperative mechanism between metallic Ag and O$_{ad}$ (oxygen atoms adjacent to the active Ag sites), and O$_{ad}$ as a Brønsted base site should play an important role in the dissociation of water. These findings demonstrate that a surface science driven strategy is useful to design a new Ag catalyst for green organic reactions involving water dissociation as a critical step.

Appendix A. Supplementary data

Supplementary data associated with this article can be found, in the online version, at doi:10.1016/j.apcata.2012.02.007.

Fig. 7. Mechanism of Ag/SiO$_2$-catalyzed hydration of nitriles.

References

[1] J. March, Advanced Organic Chemistry, Wiley-Interscience, New York, 1992, 383.
[2] T.J. Ahmed, S.M.M. Knapp, D. Tyler, Coord. Chem. Rev. 255 (2011) 949–974.
[3] T. Oshiki, H. Yamashita, K. Sawada, M. Utsunomiya, K. Takahashi, K. Takai, Organometallics 24 (2005) 6287–6290.
[4] R. García- Álvarez, J. Díez, P. Crochet, V. Cadierno, Organometallics 29 (2010) 3955–3965.
[5] C.S. Yi, T.N. Zeczycki, S.V. Lindeman, Organometallics 27 (2008) 2030–2035.
[6] W.K. Fung, X. Huang, M.L. Man, S.M. Ng, M.Y. Hung, Z. Lin, C.P. Lau, J. Am. Chem. Soc. 125 (2003) 11539–11544.
[7] C.W. Leung, W. Zheng, Z. Zhou, Z. Lin, C.P. Lau, Organometallics 27 (2008) 4957–4969.
[8] N. Toshima, Y. Wang, Chem. Lett. 22 (1993) 1611–1614.
[9] A. Ishizuka, Y. Nakazaki, T. Oshiki, Chem. Lett. 38 (2009) 360–361.
[10] H. Miura, K. Sugiyama, S. Kawakami, T. Aoyama, T. Matsuda, Chem. Lett. 11 (1982) 183–186.
[11] K. Sugiyama, H. Miura, Y. Watanabe, Y. Ukai, T. Matsuda, Bull. Chem. Soc. Jpn. 60 (1987) 1579–1583.
[12] K. Yamaguchi, M. Matsushita, N. Mizuno, Angew. Chem. Int. Ed. 43 (2004) 1576–1580.
[13] S.C. Roy, P. Dutta, L.N. Nandy, S.K. Roy, P. Samuel, S.M. Pillai, V.K. Kaushik, M. Ravindranathan, Appl. Catal., A 290 (2005) 175–180.

[14] F. Bazi, H.E.I Badaoui, S. Tamani, S. Sokori, A. Solhy, D.J. Macquarrie, S. Sebti, Appl. Catal., A 301 (2006) 211–214.
[15] T. Mitsudome, Y. Mikami, H. Mori, S. Arita, T. Mizugaki, K. Jitsukawa, K. Kaneda, Chem. Commun. 45 (2009) 3258–3260.
[16] V. Polshettiwar, R.S. Varma, Chem. Eur. J. 15 (2009) 1582–1586.
[17] S. Ichikawa, S. Miyazoe, O. Matsuoka, Chem. Lett. 40 (2011) 512–513.
[18] M. Tamura, H. Wakasugi, K. Shimizu, A. Satsuma, Chem. Eur. J. 17 (2011) 11428–11431.
[19] I.E. Wachs, Surf. Sci. 544 (2003) 1–4.
[20] M. Naodovic, H. Yamamoto, Chem. Rev. 108 (2008) 3132–3181.
[21] T. Mitsudome, S. Arita, H. Mori, T. Mizugaki, K. Jitsukawa, K. Kaneda, Angew. Chem. Int. Ed. 47 (2008) 138–141.
[22] K. Shimizu, K. Sawabe, A. Satsuma, Catal. Sci. Technol. 1 (2011) 331–341.
[23] Y. Zhang, J.L. Whitten, J. Phys. Chem. A 112 (2008) 6358–6363.
[24] J.L.C. Fajín, M.N.D.S. Cordeiro, F. Illas, J.R.B. Gomes, J. Catal. 276 (2010) 92–100.
[25] A. Montoya, B. Haynes, J. Phys. Chem. C 111 (2007) 1333–1341.
[26] G. Wang, S. Xia, X. Bu, J. Catal. 244 (2006) 10–16.
[27] M. Bowker, M.A. Barteau, R.J. Madix, Surf. Sci. 92 (1980) 528–548.
[28] O. Nakagoe, N. Takagi, K. Watanabe, Y. Matsumoto, Phys. Chem. Chem. Phys. 9 (2007) 5274–5278.
[29] W. Klopper, J.G.C.M. van Duijneveldt-van de Rijdt, F.B. van Duijneveldt, Phys. Chem. Chem. Phys. 2 (2000) 2227–2234.
[30] H. Olcay, L. Xu, Y. Xu, G.W. Huber, ChemCatChem 12 (2010) 1420–1424.
[31] C.-B. Wang, G. Deo, I.E. Wachs, J. Phys. Chem. B 103 (1999) 5645–5656.
[32] N. Iwasaki, Y. Sasaki, Y. Nishina, Surf. Sci. 198 (1988) 524–540.
[33] E.R. Savinova, P. Kraft, B. Pettinger, K. Doblhofer, J. Electroanal. Chem. 430 (1997) 47–56.
[34] X. Bao, M. Muhler, B. Pettinger, R. Schlögl, G. Ertl, Catal. Lett. 22 (1993) 215–225.
[35] Y. Cao, Z.-X. Chen, Surf. Sci. 600 (2006) 4572–4583.
[36] A. Shavorskiy, M.J. Gladys, G. Held, Phys. Chem. Chem. Phys. 10 (2008) 6150–6159.
[37] M. Pan, S. Hoang, C.B. Mullins, Catal. Today 160 (2011) 198–203.
[38] J.L. Gong, C.B. Mullins, Acc. Chem. Res. 42 (2009) 1063–1073.
[39] B. Xu, L. Zhou, R.J. Madix, C.M. Friend, Angew. Chem. Int. Ed. 49 (2010) 394–398.